

Supplementary Material

Effect of Potassium Doping on Electronic Structure and Thermoelectric Properties of Topological Crystalline Insulator

Subhajit Roychowdhury,¹ U. Sandhya Shenoy,² Umesh V. Waghmare² and Kanishka Biswas^{1,a)}

¹*New Chemistry Unit and ²Theoretical Sciences Unit, Jawaharlal Nehru Centre for Advanced Scientific Research (JNCASR), Jakkur P.O., Bangalore 560 064, India.*

a) Authors to whom correspondence should be addressed. Electronic address:
kanishka@jncasr.ac.in

EXPERIMENTAL & THEORETICAL DETAILS

Reagents: Tin (Sn, Alfa Aesar 99.99+ %), tellurium (Te, Alfa Aesar 99.999+ %), lead (Pb, Alfa Aesar 99.99+ %) and potassium (K, Sigma Aldrich 99.5 %) were used for synthesis without further purification.

Synthesis: Ingots (~6 g) of $Pb_{0.60-x}K_xSn_{0.40}Te$ ($x = 0.0, 0.01, 0.02, 0.03, 0.04$) were synthesized by mixing appropriate ratios of high-purity elemental Sn, Pb, K and Te in carbon coated quartz tubes. The tubes were sealed under vacuum (10^{-5} Torr) and slowly heated to 723 K over 12 hrs, then heated up to 1323 K in 5 hrs, annealed for 5 hrs, and cooled down to 1023 K over 2 hrs and annealed for 4 hrs, then slowly cool down to room temperature over a period of 18 hrs. We have performed thermoelectric experiments for all samples as synthesized ingot from melt (after cutting and polishing it to required dimension).

Powder X-ray diffraction: Powder X-ray diffraction of samples were recorded using a Cu K α ($\lambda = 1.5406$ Å) radiation on a Bruker D8 diffractometer.

Band gap measurement: To estimate optical band gap of the as synthesized samples diffuse measurement has been done with finely grinded powder at room temperature using FT-IR Bruker IFS 66V/S spectrometer in a wave-number range $4000\text{-}400$ cm^{-1} with 2 cm^{-1}

resolution and 50 scans. Absorption (α/S) data were calculated from reflectance data using Kubelka-Munk equation: $\alpha/S = (1-R)^2/(2R)$, where R is the reflectance, α and S are the absorption and scattering coefficient, respectively. The energy band gaps were derived from α/S vs E (eV) plot.

Electrical Transport: Electrical conductivity and Seebeck coefficients were measured simultaneously under He atmosphere from room temperature to 723 K on a ULVAC-RIKO ZEM-3 instrument system. The typical sample for measurement had a parallelepiped shape with the dimensions of $\sim 2 \times 2 \times 8$ mm³. The longer direction coincides with the direction in which the thermal conductivity was measured.

Hall Measurement: To determine carrier concentration, Hall measurements have been carried out using Van der-Pauw method, in a magnetic field of 0.58 T at room temperature (RT) in ECOPIA Hall effect measurement system (HMS 3000).

Thermal transport: Thermal diffusivity, D , was directly measured in the range 300–723 K by using a laser flash diffusivity method in a Netzsch LFA-457 (see the D vs. T data for all samples in Fig. S1, Electronic Supporting Information, ESI). Coins with ~ 8 mm diameter and ~ 2 mm thickness were used in all of the measurements. The temperature dependent heat capacity, C_p , was derived using a standard sample (pyroceram) in LFA-457. The total thermal conductivity, κ_{total} , was calculated using the formula, $\kappa_{\text{total}} = DC_p\rho$, where ρ is the density of the sample, measured using the Archimedes method. The density of the pellets obtained was in the range $\sim 97\%$ of the theoretical density. Thermal conductivity was measured in the same direction of electronic transport measurement.

Computational details: Density Functional Theoretical (DFT) calculations were performed to determine the electronic structure K substituted Pb₁₀Sn₆Te₁₆ using Quantum Espresso package.¹ Effect of the spin-orbit coupling was included in determination of realistic

electronic structure since Pb, Sn and Te have high atomic numbers and atomic masses, and the associated relativistic effects cannot be neglected. For this purpose, valence and semicore electronic states of Pb, Sn, Te and K ($5d^{10} 6s^2 6p^2$, $4d^{10} 5s^2 5p^2$, $4d^{10} 5s^2 5p^4$ and $4s^1$ respectively) were treated with fully relativistic ultra-soft pseudopotentials. The exchange-correlation energy functional was approximated within a Generalized Gradient Approximation (GGA) with parametrized form of Perdew, Burke, and Erzenhoff (PBE).² PbTe and SnTe are known to crystallize in the rocksalt structure with two atoms per unit cell with symmetry given by $Fm\bar{3}m$ space group. To simulate substitutional doping a ($\sqrt{2} \times \sqrt{2} \times 2$) a_0 supercell of K doped $Pb_{1-x}Sn_xTe$ containing 32 atoms was used. A 7X7X5 uniform grid of k-points was used in sampling integrations over the Brillouin-zone of the supercell. Energy cutoffs of 40 Ry and 320 Ry were used in truncation of the plane wave basis used for representing wavefunctions and charge density, respectively. Gaussian smearing with a width of 0.003 eV was used to smear the Fermi surface discontinuity in occupation numbers of electronic states. Electronic structure of $Pb_9Sn_6KTe_{16}$ was determined along high symmetry lines ($\Gamma - X - M - \Gamma - Z - R - A - Z$) in the Brillouin zone, at the experimental lattice constant of 6.3953 Å for ~6 % K doped system.

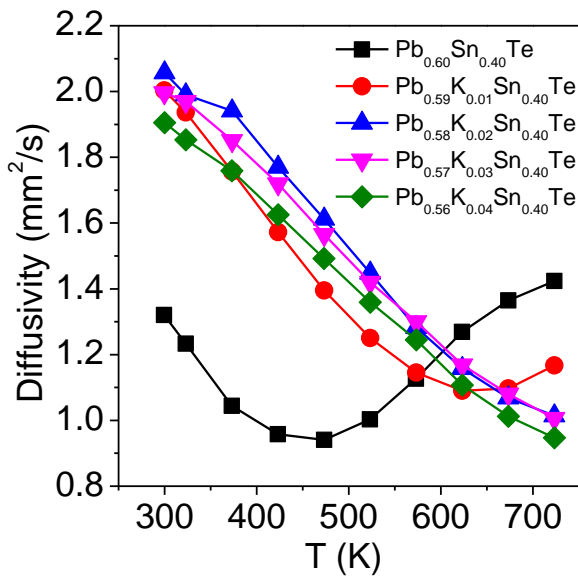


Fig. S1. Temperature dependent thermal diffusivity of $\text{Pb}_{0.60-x}\text{K}_x\text{Sn}_{0.40}\text{Te}$ ($x = 0.0, 0.01, 0.02, 0.03, 0.04$) samples.

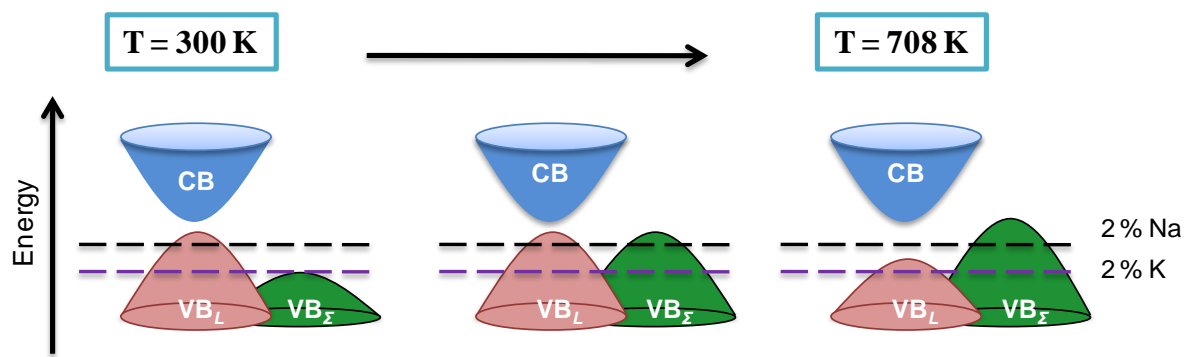


Fig. S2. Schematic of the electronic structure of $\text{Pb}_{0.6-x} \text{M}_{0.02} \text{Sn}_{0.4}\text{Te}$ (M = Na, K) at different temperature.

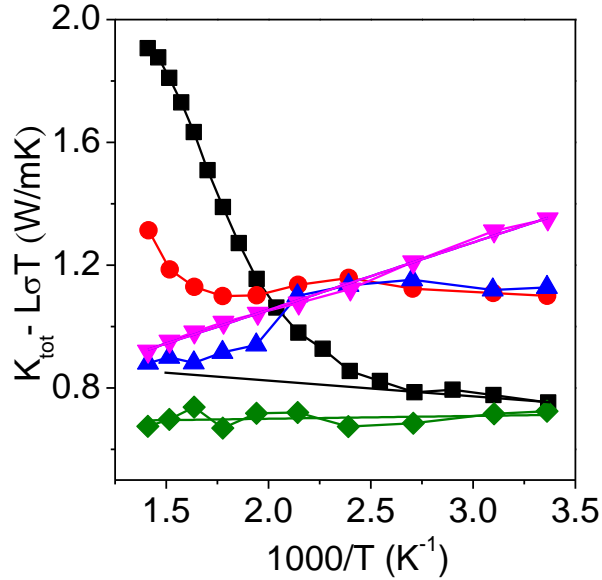


Fig. S3. The difference of total and electronic thermal conductivity $\{\kappa_{\text{total}} - \kappa_{\text{el}}(L\sigma T)\}$ as a function of temperature. The solid line is linear fitting to the lattice thermal conductivity in the 300-710 K range. Deviation from linear region indicates a significant contribution bipolar thermal conductivity (κ_{bi}).³

At high temperature the minority carriers generated in intrinsic excitations not only decrease the Seebeck coefficient, but also increase the thermal conductivity due to the bipolar diffusion. If the bipolar diffusion takes place in semiconductor, generally the lattice thermal conductivity (κ_{lat}) can be overestimated since an extra term (bipolar thermal conductivity, κ_{bi}) contributes to the total thermal conductivity. Therefore, the total thermal conductivity κ_{total} is given by:

$$\kappa_{\text{total}} = \kappa_{\text{lat}} + \kappa_{\text{el}} + \kappa_{\text{bi}}$$

In order to quantify the contribution of bipolar thermal conductivity (κ_{bi}) at high temperature, the κ_{bi} is separated from the κ_{total} according to the previously reported method.^{4,5} The difference, $\kappa_{\text{total}} - \kappa_{\text{el}}$, as a function of T^{-1} is shown in Fig. S3. Since the acoustic phonon scattering is predominant at low temperatures before bipolar diffusion is significant, $\kappa_{\text{total}} - \kappa_{\text{el}}$ equals to κ_{lat} , which is proportional to T^{-1} .

As the temperature is increased to ~ 425 K, the $\kappa_{\text{total}} - \kappa_{\text{el}}$ starts to gradually deviate from a linear relationship between κ_{lat} and T^{-1} because the bipolar diffusion starts to contribute to the thermal conductivity.

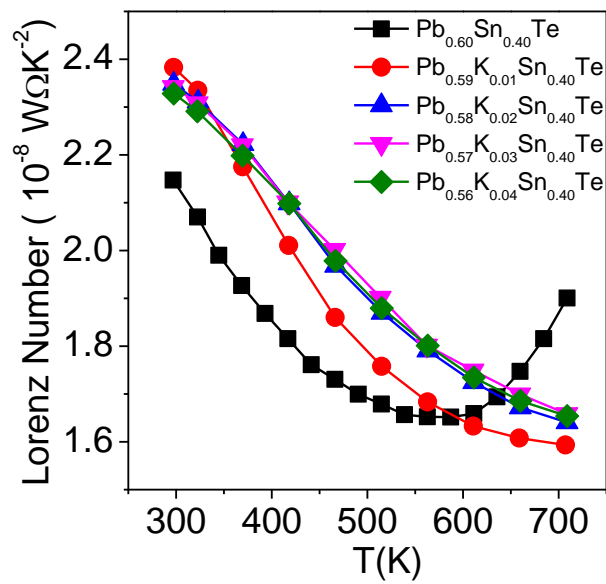


Fig. S4. Temperature dependent Lorenz number (L) of $\text{Pb}_{0.60-x}\text{K}_x\text{Sn}_{0.40}\text{Te}$ ($x = 0.0, 0.01, 0.02, 0.03, 0.04$) samples.

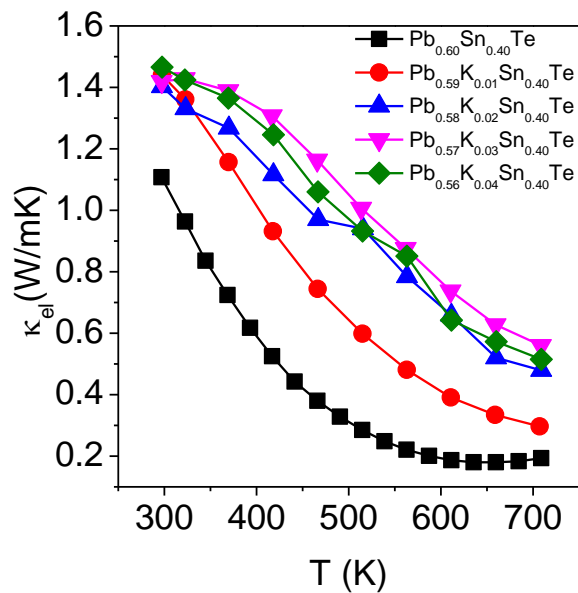


Fig. S5. Temperature dependent electronic thermal conductivity (κ_{el}) of $\text{Pb}_{0.60-x}\text{K}_x\text{Sn}_{0.40}\text{Te}$ ($x = 0.0, 0.01, 0.02, 0.03, 0.04$) samples.

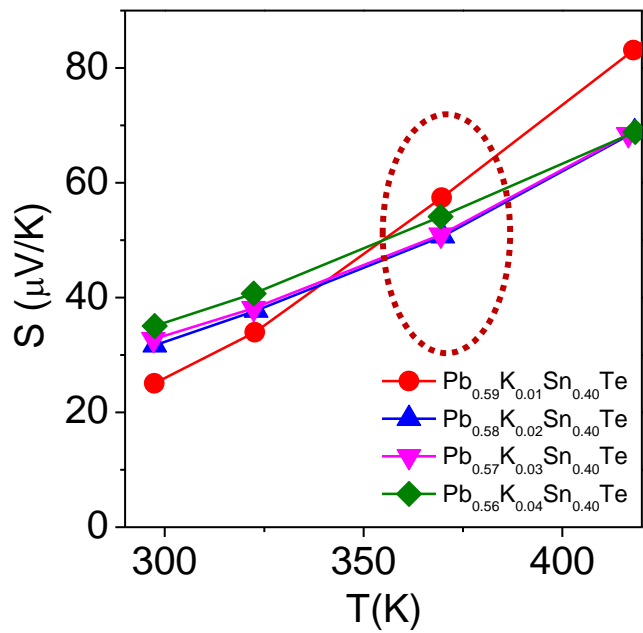


Fig. S6. Zoomed version of temperature dependent Seebeck coefficient values in the range of 290 K – 420 K for $\text{Pb}_{0.60-x}\text{K}_x\text{Sn}_{0.40}\text{Te}$ ($x = 0.01, 0.02, 0.03, 0.04$) samples.

Table S1. Band gaps around high-symmetric (Γ) point for both Na and K doped $\text{Pb}_{0.60}\text{Sn}_{0.40}\text{Te}$.

	Electronic gap (eV)	
	Na doped TCI	K doped TCI
$\Delta E_{\Gamma-\delta}$	0.037	0.034
ΔE_{Γ}	0.187	0.163

¹P. Giannozzi, S. Baroni, N. Bonini, M. Calandra, R. Car, C. Cavazzoni, D. Ceresoli, G. L. Chiarotti, M. Cococcioni, I. Dabo, A. L. Corso, S. de. Gironcoli, S. Fabris, G. Fratesi, R. Gebauer, U. Gerstmann, C. Gougoussis, A. Kokalj, M. Lazzeri, L. Martin-Samos, N. Marzari, F. Mauri, R. Mazzarello, S. Paolini, A. Pasquarello, L. Paulatto, C. Sbraccia, S. Scandolo, G. Sclauzero, A. P. Seitsonen, A. Smogunov, P. Umari, and R. M. Wentzcovitch, *J. Phys. Condens. Matter.* **21**, 395502 (2009).

²J. P. Perdew, K. Burke, and M. Ernzerhof, *Phys. Rev. Lett.* **77**, 3865 (1996).

³L. D. Zhao, H. J. Wu, S. Q. Hao, C. I. Wu, X. Y. Zhou, K. Biswas, J. Q. He, T. P. Hogan, C. Uher, C. Wolverton, V. P. Dravid, and M. G. Kanatzidis, *Energy Environ. Sci.* **6**, 3346 (2013).

⁴H. Kitagawa, M. Wakatsuki, H. Nagaoka, H. Noguchi, Y. Isoda, K. Hasezaki, and Y. Noda, *J. Phys. Chem. Solids* **66**, 1635 (2005).

⁵W. S. Liu, B. P. Zhang, J. F. Li, H. L. Zhang, and L. D. Zhao, *J. Appl. Phys.* **102**, 103717 (2007).